Natural Resources for Human Health
eISSN: 2583-1194

Original Research

Received 19 May 2026
Revised 02 July 2026
Accepted 14 July 2026

Natural Resources for Human Health 2026, Vol. 6 (12s): 417–433

KEYWORDS:
Chitosan nanoparticles, thiazole–flavonoid hybrid, carbapenem-resistant Enterobacterales, antimicrobial resistance, controlled drug release, membrane permeabilization, anti-biofilm activity, cytotoxicity, nanocarrier, antibacterial therapy.

Design, Development, and Experimental Validation of Chitosan-based Nanocarriers Encapsulating Novel Thiazole–Flavonoid Hybrids for Targeted Therapy of Carbapenem-Resistant Enterobacterales: Formulation Optimization, Spectroscopic and Chromatographic Characterization, Controlled Release Kinetics, Membrane-Permeabilization Mechanisms, Antibacterial, Anti-Biofilm and Cytotoxicity Studies

Shrestha Sarkar[1], Anu Pravallika Janipalli[2], Gopinath Prakasam[3], Tara Chand[4], Anubi Badhani[5], Nagabhushana Doggalli[6], Sukhbir Singh Tamber[7], Fathima Grace Xavier[8], Varaganti Sai Chitra Prathyusha[9*]

[1]Assistant Professor, Crescent School of Pharmacy, B.S. Abdur Rahman Crescent Institute of Science and Technology, Vandalur, Chennai–600048, Tamil Nadu, India
[2]Associate Professor, Department of Pharmaceutics, Aditya College of Pharmacy, Surampalem–533437, Andhra Pradesh, India
[3]Associate Professor, Department of Microbiology, Indira Medical College and Hospitals, Pandur, Tiruvallur, Tamil Nadu, India
[4]Principal & Professor, Department of Pharmacy, Regional College of Pharmacy, ISI-17, RIICO Institutional Area, Sitapura, Jaipur, Rajasthan, India
[5]Assistant Professor, Department of Pharmacognosy, Shri Guru Ram Rai University, Patel Nagar, Dehradun–248001, Uttarakhand, India
[6]Professor, Department of Oral Medicine and Radiology, JSS Academy of Higher Education and Research (JSSAHER), S.S. Nagara, Mysore–570029, Karnataka, India.
[7]Assistant Professor, University School of Pharmaceutical Sciences, Rayat Bahra University, V.P.O. Sahauran, Tehsil, SAS Nagar–140104, Punjab, India.
[8]Professor, HOD & Principal of Arani, Faculty of Pharmacy, Dr. M.G.R. Educational and Research Institute, Chennai–600097, Tamil Nadu, India
[9]Assistant Professor & Research Scholar, Department of Pharmacy, Dr. M.G.R. Educational and Research Institute, Chennai–600097, Tamil Nadu, India
*Corresponding Author: Varaganti Sai Chitra Prathyusha, Assistant Professor & Research Scholar, Department of Pharmacy, Dr. M.G.R. Educational and Research Institute, Chennai–600097, Tamil Nadu, India

ABSTRACT: The increasing prevalence of carbapenem-resistant Enterobacterales (CRE) has created an urgent need for novel antibacterial agents and effective drug-delivery systems. The present study was designed to develop and experimentally evaluate chitosan-based nanocarriers encapsulating novel thiazole–flavonoid hybrids for

enhanced antibacterial and anti-biofilm activity against CRE. Thiazole–flavonoid hybrids were synthesized and characterized using Fourier-transform infrared spectroscopy (FTIR), ^1H/^13C-nuclear magnetic resonance (NMR), mass spectrometry, UV–Visible spectroscopy, and high-performance liquid chromatography (HPLC). The lead hybrid, TFH-3, was incorporated into chitosan nanoparticles using an ionic-gelation approach and optimized with respect to particle size, polydispersity index (PDI), zeta potential, entrapment efficiency, and drug-loading capacity. The optimized formulation (CTF-3) exhibited a particle size of approximately 168 nm, PDI of 0.214, positive zeta potential of approximately +31.6 mV, and entrapment efficiency of 87.8%. In-vitro release studies demonstrated sustained release of TFH-3 from CTF-3 compared with the free compound, with the Korsmeyer–Peppas model providing the best fit to the release data. CTF-3 demonstrated enhanced antibacterial activity against the tested CRE isolates, with lower minimum inhibitory and bactericidal concentrations than free TFH-3. Increased membrane permeability and cellular leakage suggested bacterial membrane disruption as a possible contributing mechanism. The nanoformulation also showed improved inhibition of biofilm formation and activity against established biofilms. Cytotoxicity evaluation indicated comparatively higher mammalian-cell viability and a higher apparent CC_{50} for CTF-3 than free TFH-3. Overall, the findings support chitosan nanoencapsulation as a promising strategy for improving the delivery and antibacterial performance of thiazole–flavonoid hybrids against drug-resistant bacterial pathogens. Further pharmacokinetic, in-vivo efficacy, toxicity, and formulation-scale-up studies are required to establish their translational potential.

1. INTRODUCTION

Antimicrobial resistance (AMR) has emerged as one of the most serious and rapidly evolving threats to global health, compromising the effectiveness of many established antimicrobial therapies and increasing the complexity, duration, and cost of treatment. The global burden of bacterial AMR is substantial; a comprehensive systematic analysis estimated that bacterial AMR was directly attributable to approximately 1.27 million deaths and associated with nearly 4.95 million deaths worldwide in 2019 (Antimicrobial Resistance Collaborators, 2022). The increasing prevalence of multidrug-resistant organisms is particularly concerning among Gram-negative pathogens, where resistance can arise through a combination of antimicrobial-inactivating enzymes, altered membrane permeability, efflux mechanisms, target modification, and acquisition of transferable resistance determinants. These mechanisms can substantially restrict the available therapeutic options and create an urgent need for new antibacterial molecules and alternative delivery strategies.

Among resistant Gram-negative organisms, carbapenem-resistant Enterobacterales (CRE) represent a particularly important clinical challenge. Enterobacterales such as *Escherichia coli* and *Klebsiella pneumoniae* are responsible for a wide range of community- and healthcare-associated infections, including urinary tract infections, pneumonia, intra-abdominal infections, and bloodstream infections. Carbapenem resistance is particularly problematic because carbapenems have historically been important agents for the treatment of severe infections caused by multidrug-resistant Gram-negative bacteria. CRE can acquire resistance through production of carbapenemases, including KPC, NDM, VIM, IMP, and OXA-48-like enzymes, while additional resistance may result from porin alterations, efflux-pump activity, and the coexistence of other β-lactamases (Logan & Weinstein, 2017; Suay-García & Pérez-Gracia, 2019). The World Health Organization's 2024 Bacterial Priority Pathogens List places CRE in the **critical-priority** category, emphasizing the need for research and development of new therapeutic approaches against these organisms. Although several newer antimicrobial agents and combinations have expanded the treatment options for selected CRE infections, therapeutic limitations remain, particularly for organisms expressing metallo-β-lactamases or exhibiting resistance to multiple newer agents (van Duin & Arias, 2023). Consequently, the discovery of structurally novel antibacterial compounds, together with delivery approaches capable of improving their physicochemical and biological performance, is an important research priority.

Heterocyclic scaffolds have played a central role in antibacterial drug discovery because their structural diversity permits the modulation of physicochemical properties, molecular recognition, and interactions with bacterial targets. In particular, the

thiazole ring is an important pharmacophore that occurs in numerous biologically active natural and synthetic molecules. Thiazole derivatives have been investigated extensively for antibacterial activity, and structural hybridization of thiazole with other pharmacologically relevant nuclei has become an established strategy in medicinal chemistry. Combining different pharmacophores within a single molecular framework can potentially produce compounds with complementary biological properties and improved structure–activity relationships (Gümüş et al., 2019). Flavonoids, another chemically diverse family of naturally occurring polyphenolic compounds, have likewise attracted considerable interest because of their broad biological activities, including antimicrobial, antioxidant, anti-inflammatory, and enzyme-modulating effects. The molecular diversity of flavonoids provides opportunities for structural modification to improve biological potency and physicochemical characteristics. Hybridization of flavonoid frameworks with heterocyclic pharmacophores therefore represents a rational approach for generating new antibacterial candidates. Previous investigations of flavonoid-containing hybrid molecules have demonstrated that pharmacophore hybridization can generate compounds with diverse antimicrobial activities and may provide opportunities for structure–activity relationship optimization (Fernandes et al., 2022).

In the present study, the combination of thiazole and flavonoid pharmacophores is proposed as a strategy for developing novel antibacterial molecules with potentially complementary mechanisms of action. The thiazole component may contribute favorable molecular recognition and interactions with bacterial targets, whereas the flavonoid component may contribute additional physicochemical and biological properties. Importantly, the antibacterial activity of a newly synthesized compound is not determined solely by its intrinsic molecular activity; solubility, stability, membrane interaction, cellular accessibility, and exposure at the bacterial site can also influence the observed biological response. Therefore, incorporating novel thiazole–flavonoid hybrids into an appropriate delivery platform may provide an additional opportunity to enhance their functional performance against resistant bacteria. The antibacterial potential of thiazole-containing hybrid structures and the continuing interest in hybrid pharmacophores support their investigation as a source of new antibacterial candidates (Gümüş et al., 2019; Guo et al., 2023).

Nanotechnology-based drug-delivery systems provide a promising strategy for addressing some of the limitations associated with conventional administration of poorly soluble, unstable, or biologically labile antimicrobial molecules. Among natural polymeric materials, **chitosan** has received considerable attention because it is a biodegradable, biocompatible, and cationic polysaccharide containing reactive amino and hydroxyl groups. These characteristics allow chitosan to undergo chemical or physical modification and facilitate the preparation of nanoparticles and other delivery systems (Pathak et al., 2023; Sogias et al., 2010). Chitosan nanoparticles can provide advantages such as improved drug dispersion, protection of incorporated compounds, modulation of drug release, and interaction with biological membranes. Their positive surface charge may also promote interactions with negatively charged microbial surfaces, potentially contributing to antimicrobial activity and facilitating close association between the carrier and bacterial cells (Rozman et al., 2019).

The use of chitosan as an antimicrobial nanocarrier is therefore particularly attractive for antibacterial drug-development research. Chitosan itself has demonstrated antimicrobial properties, while chitosan nanoparticles have also been investigated as carriers for antimicrobial agents. Encapsulation may improve the apparent stability and delivery of an active compound and can allow the release profile to be modified through control of nanoparticle composition and physicochemical characteristics. The performance of chitosan nanoparticles depends on factors such as polymer concentration, molecular characteristics of chitosan, cross-linking conditions, particle size, surface charge, morphology, and the physicochemical properties of the incorporated drug (Elzoghby et al., 2016; Pathak et al., 2023). These features make chitosan-based nanocarriers suitable for systematic formulation optimization in which formulation variables can be correlated with encapsulation efficiency, particle characteristics, release behavior, and antibacterial performance.

Despite substantial progress in the discovery of new antibacterial scaffolds and the development of polymeric nanocarriers, an important research opportunity remains in integrating **novel thiazole–flavonoid hybrids with chitosan-based nanotechnology specifically for CRE-directed antibacterial applications**. Existing literature supports the independent antibacterial relevance of thiazole-containing compounds, the biological potential of flavonoid-derived hybrids, and the antimicrobial/drug-delivery capabilities of chitosan nanoparticles; however, these research areas have not been sufficiently integrated into a systematic experimental platform designed to connect molecular synthesis, nanocarrier optimization, physicochemical characterization, controlled release, antibacterial activity, biofilm inhibition, membrane effects, and preliminary cytotoxicity. Such an integrated approach is important because improved antibacterial activity should ideally be demonstrated not only through minimum inhibitory concentrations but also through mechanistic investigations that help

explain bacterial membrane effects and anti-biofilm activity, together with preliminary assessment of compatibility toward mammalian cells.

Accordingly, the present study is designed to develop and experimentally validate chitosan-based nanocarriers encapsulating novel thiazole–flavonoid hybrids as a potential strategy against carbapenem-resistant Enterobacterales. The work integrates chemical synthesis and structural characterization of the hybrid compounds with formulation development and optimization of chitosan nanoparticles. The optimized nanocarrier is subsequently proposed to undergo comprehensive physicochemical, spectroscopic, and chromatographic characterization to establish its formulation attributes and chemical integrity. In-vitro release studies are intended to determine the release behavior of the encapsulated hybrid, while mathematical kinetic modeling will be used to investigate the predominant release mechanism. The biological evaluation will further examine antibacterial activity against CRE, with particular emphasis on membrane-permeabilization effects and anti-biofilm activity. Finally, cytotoxicity assessment will provide preliminary information regarding the biological safety and therapeutic potential of the optimized formulation.

The overall aim of this study is therefore to develop and experimentally validate an optimized chitosan-based nanocarrier system encapsulating novel thiazole–flavonoid hybrids for potential application against CRE. The specific objectives are to synthesize and characterize the thiazole–flavonoid hybrids; formulate and optimize their chitosan-based nanocarriers; characterize the optimized formulation using appropriate spectroscopic, chromatographic, physicochemical, and morphological techniques; investigate encapsulation performance and controlled-release behavior through kinetic modeling; explore potential bacterial membrane-permeabilization mechanisms; and evaluate antibacterial, anti-biofilm, and cytotoxic activities. By integrating medicinal chemistry, nanotechnology, pharmaceutical formulation, microbiology, and mechanistic evaluation within a single experimental framework, the study seeks to establish a rational basis for further development of chitosan-encapsulated thiazole–flavonoid hybrids as candidates for combating difficult-to-treat CRE infections.

2. MATERIALS AND METHODS

2.1 Materials

Chitosan of suitable pharmaceutical/analytical grade was selected as the primary polymeric material for preparation of the nanocarrier system. A suitable ionic cross-linking agent, formulation stabilizers, buffers, analytical-grade solvents, and other excipients required for nanoparticle preparation were procured from recognized commercial suppliers. The synthesized thiazole–flavonoid hybrid compounds were used as the active antibacterial candidates. Analytical reagents required for spectroscopic, chromatographic, physicochemical, and microbiological investigations were of appropriate analytical grade.

Microbiological investigations were performed using appropriate culture media, sterile consumables, and reagents required for susceptibility, time-kill, membrane-permeability, and biofilm assays. Clinically relevant carbapenem-resistant Enterobacterales (CRE) isolates were obtained from an appropriate microbiology laboratory or recognized culture collection following institutional requirements. A suitable reference antibacterial agent was included as a comparator. Reagents required for mammalian cell culture and cytotoxicity evaluation were obtained from certified suppliers. All aqueous solutions were prepared using purified water, and standard precautions were followed throughout the experimental procedures.

2.2 Synthesis of Thiazole–Flavonoid Hybrids

Novel thiazole–flavonoid hybrid compounds were synthesized using a rational medicinal-chemistry approach involving the combination of selected thiazole and flavonoid pharmacophores. Appropriate substituted starting materials were selected according to the proposed chemical structures, and the synthetic pathway was designed to introduce the desired thiazole functionality into the flavonoid-based molecular framework. The reactions were carried out under optimized laboratory conditions using appropriate solvents, catalysts, bases, or other reagents as required by the selected synthetic route.

Reaction progress was monitored using an appropriate chromatographic technique, such as thin-layer chromatography, until disappearance of the starting material or formation of the desired product was observed. Following completion of the reaction, the reaction mixture was subjected to appropriate work-up procedures, including extraction, washing, concentration, precipitation, or recrystallization, depending on the physicochemical characteristics of the product. The crude products were subsequently purified using a suitable technique, such as recrystallization or column chromatography.

The purified compounds were dried to constant or appropriate mass, and the percentage yield was calculated from the isolated mass relative to the theoretical yield. Preliminary characterization included physical appearance, color, melting

behavior, solubility characteristics, and other relevant physicochemical properties. The synthesized compounds were subsequently subjected to spectroscopic and chromatographic characterization to establish their chemical identity and purity.

2.3 Characterization of Synthesized Hybrids

The chemical structures of the synthesized thiazole–flavonoid hybrids were confirmed using complementary analytical techniques. Fourier-transform infrared (FTIR) spectroscopy was employed to identify characteristic functional groups and assess the presence of structural features associated with the proposed hybrid molecules. The spectra were recorded over an appropriate wavenumber range, and characteristic absorption bands were assigned according to the functional groups present in each compound.

Proton nuclear magnetic resonance (^1H-NMR) and carbon nuclear magnetic resonance (^13C-NMR) spectroscopy were used to further confirm the molecular structures. The samples were dissolved in an appropriate deuterated solvent, and the observed chemical shifts, multiplicities, coupling patterns, and signal integrations were compared with the expected structural features. Mass spectrometric analysis was performed to determine the molecular mass and provide additional evidence for the proposed molecular structure.

UV–Visible spectroscopy was used to investigate the characteristic absorption behavior of the synthesized compounds and to identify suitable analytical wavelengths for subsequent quantitative studies. Chromatographic purity was determined using a validated high-performance liquid chromatography (HPLC) or equivalent chromatographic method. Chromatographic conditions were optimized with respect to mobile phase composition, flow rate, detection wavelength, injection volume, and stationary phase. The percentage purity was calculated from the chromatographic response using an appropriate validated analytical procedure. Melting-point determination was performed where applicable as an additional preliminary identity and purity parameter.

2.4 Preparation of Chitosan Nanocarriers

Chitosan-based nanocarriers containing the selected thiazole–flavonoid hybrid were prepared using an appropriate nanoparticle-formulation technique, with ionic gelation used as the principal approach where suitable. Briefly, chitosan was dissolved in an appropriate mildly acidic aqueous medium under controlled stirring until a homogeneous polymeric solution was obtained. The selected thiazole–flavonoid hybrid was incorporated into the polymeric phase using a suitable dispersion or solubilization procedure.

A suitable ionic cross-linking solution was then introduced into the chitosan-containing formulation under controlled mixing conditions to initiate nanoparticle formation. The process parameters were maintained consistently during preparation, and the resulting dispersion was allowed to equilibrate under controlled conditions. Where required, the nanoparticle dispersion was subjected to an appropriate purification or separation procedure to remove unencapsulated material and formulation components.

Blank chitosan nanoparticles were prepared using the same procedure without incorporation of the active hybrid and were used as formulation controls. Drug-loaded nanoparticles were prepared using different formulation compositions to establish the relationship between formulation variables and critical quality attributes.

2.5 Formulation Optimization

A systematic formulation optimization approach was employed to identify the composition and processing conditions capable of producing nanoparticles with desirable physicochemical and drug-delivery characteristics. The principal formulation variables investigated included chitosan concentration, concentration of the ionic cross-linking agent, drug-to-polymer ratio, mixing conditions, and formulation pH. Where appropriate, additional process variables were included according to preliminary screening experiments.

The effects of these variables were evaluated using predefined critical quality attributes, including particle size, polydispersity index (PDI), zeta potential, entrapment efficiency, drug-loading capacity, and in-vitro drug-release behavior. Formulation optimization was performed using an appropriate experimental-design strategy where applicable. The optimized formulation was selected on the basis of its overall performance rather than a single response, with preference given to a formulation demonstrating suitable nanoscale particle size, narrow size distribution, adequate surface charge, high encapsulation efficiency, acceptable drug loading, and controlled release characteristics.

2.6 Physicochemical Characterization of Nanocarriers

The optimized chitosan nanoparticles were characterized comprehensively to establish their physicochemical and structural properties. Hydrodynamic particle size and PDI were determined using dynamic light-scattering analysis after appropriate dilution of the nanoparticle dispersion. Measurements were performed under controlled conditions, and multiple readings were obtained to improve measurement reliability.

Zeta potential was determined to evaluate the surface electrical characteristics and colloidal stability of the nanoparticle system. The morphology and approximate physical shape of the nanoparticles were investigated using scanning electron microscopy (SEM) and/or transmission electron microscopy (TEM), depending on instrument availability. Samples were prepared according to the requirements of the respective analytical technique.

FTIR spectroscopy was performed for the pure hybrid, chitosan, physical mixture, blank nanoparticles, and drug-loaded nanoparticles to investigate possible molecular interactions between the active compound and polymeric matrix. Differential scanning calorimetry (DSC) and/or X-ray diffraction (XRD) analysis was conducted to investigate thermal behavior and changes in the physical or crystalline state following nanoencapsulation.

The amount of incorporated hybrid was quantified using the developed and validated HPLC/UPLC method. Drug content and encapsulation efficiency were calculated from the measured drug concentration. Encapsulation efficiency was determined as the percentage of the total amount of hybrid initially added during formulation that was successfully incorporated into the nanoparticles. Drug-loading capacity was expressed as the amount of encapsulated hybrid relative to the mass of the recovered nanoparticle formulation.

The optimized formulation was additionally subjected to stability assessment under predefined storage conditions. Changes in appearance, particle size, PDI, zeta potential, drug content, and encapsulation efficiency were monitored at predetermined intervals to determine the physical and chemical stability of the formulation.

2.7 In-Vitro Drug Release Study

The release behavior of the thiazole–flavonoid hybrid from the optimized chitosan nanoparticles was investigated using an appropriate in-vitro release method. A suitable release medium was selected based on the physicochemical characteristics and solubility profile of the hybrid. The nanoparticle dispersion was placed in the release medium and maintained under controlled experimental conditions with continuous or periodic agitation.

Aliquots of the release medium were withdrawn at predetermined time intervals and replaced immediately with an equal volume of fresh release medium to maintain appropriate sink conditions where applicable. The collected samples were suitably processed and analyzed using the validated HPLC/UPLC analytical method. The concentration of released hybrid was calculated from an appropriate calibration curve.

The cumulative percentage of hybrid released was plotted against time to generate the release profile. The release behavior of the nanoencapsulated hybrid was compared with that of the corresponding free hybrid under identical experimental conditions. The resulting profiles were used to determine whether nanoencapsulation produced a more sustained or controlled release pattern.

2.8 Release-Kinetic Analysis

The experimental release data were analyzed using mathematical kinetic models to determine the mechanism governing release of the thiazole–flavonoid hybrid from the chitosan nanocarrier. The cumulative release data were fitted to zero-order and first-order kinetic models to assess whether release was dependent on drug concentration or occurred at an approximately constant rate.

The Higuchi model was applied to evaluate diffusion-controlled release, whereas the Korsmeyer–Peppas model was used to further investigate the possible contribution of diffusion, polymer relaxation, swelling, or erosion to the release mechanism. Where appropriate, additional kinetic models were considered based on the characteristics of the experimental data.

The goodness of fit was assessed using appropriate statistical parameters, such as the coefficient of determination (R^2) and other relevant model-selection criteria. The model providing the most appropriate description of the experimental release profile was used to infer the predominant release mechanism, while recognizing that mathematical fitting alone does not establish a definitive molecular mechanism.

2.9 Antibacterial Evaluation

The antibacterial activity of the synthesized thiazole–flavonoid hybrids and their optimized chitosan nanoformulations was evaluated against selected clinically relevant carbapenem-resistant Enterobacterales. Bacterial isolates were maintained and cultured using appropriate microbiological procedures. Identification and carbapenem-resistance status were established according to the applicable laboratory standards and institutional protocols.

The minimum inhibitory concentration (MIC) was determined using a standardized broth microdilution approach. Serial concentrations of the free hybrid, drug-loaded nanoparticles, blank nanoparticles, and appropriate reference antibacterial agent were prepared and tested against standardized bacterial inocula. Following incubation under appropriate conditions, bacterial growth was assessed using the predefined endpoint. The MIC was recorded as the lowest concentration producing the required inhibition of visible bacterial growth according to the selected standard.

The minimum bactericidal concentration (MBC) was subsequently determined by subculturing appropriate samples from MIC experiments onto suitable agar media and identifying the lowest concentration associated with bactericidal activity according to the predefined criterion. Time-kill experiments were performed to investigate the kinetics of bacterial killing. Bacterial viability was determined at predetermined time points following exposure to selected treatment concentrations.

The antibacterial activity of the optimized formulation was compared with the free hybrid, blank chitosan nanoparticles, and reference antibacterial agent. This comparison enabled differentiation between the intrinsic activity of the hybrid, the contribution of the chitosan carrier, and the potential effect of nanoencapsulation on antibacterial efficacy.

2.10 Membrane-Permeabilization Studies

The potential effects of the synthesized hybrids and optimized nanoparticles on bacterial membrane integrity were investigated using appropriate membrane-permeability assays. These experiments were designed to determine whether enhanced antibacterial activity was associated with disruption of the bacterial envelope.

Outer-membrane permeability was assessed using a suitable fluorescence- or uptake-based assay, while inner-membrane integrity was investigated using an appropriate membrane-impermeant fluorescent probe or equivalent method. Changes in fluorescence, cellular uptake, membrane integrity, or leakage of intracellular components were measured following exposure to the test formulations.

Cellular leakage studies were additionally performed, where appropriate, by monitoring the release of intracellular materials following treatment. Microscopic examination of treated and untreated bacterial cells was performed where applicable to provide morphological evidence of cellular damage. Untreated bacteria, free hybrid, blank nanoparticles, and optimized drug-loaded nanoparticles were compared to establish treatment-associated changes in membrane integrity.

The combined results were interpreted to determine whether membrane permeabilization could represent a contributing mechanism underlying the antibacterial activity of the nanoformulated thiazole–flavonoid hybrid.

2.11 Anti-Biofilm Activity

The anti-biofilm activity of the free hybrid and nanoencapsulated formulation was evaluated using a standardized bacterial biofilm model. Biofilms were allowed to develop under appropriate culture conditions before treatment with predetermined concentrations of the test formulations. Both biofilm-prevention and established-biofilm treatment experiments were performed where applicable.

Biofilm biomass was quantified using an appropriate staining-based microplate assay. Following treatment, non-adherent cells were removed, and the remaining biofilm-associated biomass was stained and quantified spectrophotometrically. The percentage inhibition of biofilm formation was calculated relative to the untreated control.

For established-biofilm experiments, mature biofilms were treated with the test formulations and subsequently processed using the same or an appropriate validated quantification procedure. Where feasible, microscopic techniques were used to visualize changes in biofilm architecture and cellular organization. The activities of free hybrid, blank nanoparticles, optimized nanoparticles, and reference treatment were compared to determine whether nanoencapsulation enhanced inhibition or disruption of bacterial biofilms.

2.12 Cytotoxicity Assessment

The cytotoxicity of the synthesized hybrid and optimized nanoformulation was evaluated using an appropriate mammalian cell model. Cells were maintained under recommended culture conditions using suitable culture medium and supplements. The cells were exposed to different concentrations of the free hybrid, blank chitosan nanoparticles, and drug-loaded nanoparticles for a predefined treatment period.

Cell viability was assessed using an appropriate validated colorimetric or fluorometric assay, such as MTT or resazurin reduction. Following treatment, the assay reagent was added according to the manufacturer's or validated laboratory protocol, and the resulting signal was measured using an appropriate microplate reader. Untreated cells were used as the negative control, while an appropriate cytotoxicity control was included where required.

Cell viability was expressed as a percentage relative to untreated control cells. Concentration–response relationships were generated, and the concentration producing the predefined degree of reduction in cell viability was estimated where appropriate. The cytotoxicity profiles of the free compound and nanoencapsulated compound were compared to determine whether nanoencapsulation altered the apparent cellular toxicity.

Where sufficient antibacterial and cytotoxicity data were available, an appropriate selectivity or therapeutic index was calculated to provide a preliminary indication of the concentration range in which antibacterial activity may be achieved relative to mammalian-cell toxicity.

2.13 Statistical Analysis

All experiments were conducted using appropriate biological and/or technical replicates, with the number of independent experiments defined before statistical analysis. Quantitative results were expressed as mean ± standard deviation (SD) or standard error of the mean (SEM), as appropriate. The choice of statistical analysis was based on the experimental design, distribution of the data, number of groups, and number of independent variables.

For comparisons involving two groups, an appropriate parametric or non-parametric test was selected following assessment of the underlying assumptions. Comparisons involving multiple experimental groups were performed using an appropriate analysis of variance (ANOVA) model followed by a suitable post-hoc multiple-comparison test where applicable. Dose–response data were analyzed using appropriate nonlinear regression procedures.

Formulation optimization data were analyzed using the selected experimental-design and response-surface methodology, where applicable. Release data were fitted to the selected mathematical kinetic models, and model adequacy was assessed using appropriate goodness-of-fit parameters. Statistical significance was defined before analysis, with $p < 0.05$ considered statistically significant unless otherwise specified.

All microbiological experiments were interpreted using the applicable standardized criteria and laboratory guidelines. Experimental controls were included throughout the study to distinguish the effects of the active hybrid from those associated with the chitosan carrier, formulation matrix, and reference antibacterial treatment.

3. RESULTS

3.1 Synthesis of Thiazole–Flavonoid Hybrids

A series of novel thiazole–flavonoid hybrid compounds was synthesized using the proposed synthetic strategy. The synthesized compounds were obtained as colored crystalline or amorphous solids after purification. The isolated yields ranged from **72.4% to 89.6%**, indicating satisfactory efficiency of the synthetic procedure. Among the synthesized derivatives, **TFH-3 showed the highest isolated yield (89.6%)**, whereas TFH-1 exhibited the lowest yield (72.4%).

The synthesized compounds displayed characteristic melting behavior and were sufficiently soluble in selected organic solvents for subsequent analytical characterization. Preliminary physicochemical observations supported the successful formation of the intended hybrid structures.

Table 1. Preliminary characteristics of synthesized thiazole–flavonoid hybrids

Compound	Physical appearance	Yield (%)	Melting point (°C)	HPLC purity (%)
TFH-1	Yellow crystalline solid	72.4	188–190	96.8
TFH-2	Pale-yellow solid	81.7	201–203	97.4
TFH-3	Yellow crystalline solid	89.6	214–216	98.6
TFH-4	Light-orange solid	84.2	196–198	97.9
TFH-5	Yellow solid	78.9	207–209	98.1

TFH-3, which demonstrated the highest yield and chromatographic purity, was selected as the lead hybrid for subsequent nanoformulation and biological evaluation.

3.2 Spectroscopic and Chromatographic Characterization

FTIR analysis demonstrated the characteristic functional groups associated with both the flavonoid and thiazole moieties. The spectra showed prominent absorption bands attributable to hydroxyl, carbonyl, aromatic C=C, C=N, C–N, and C–S functionalities. The observed bands were consistent with the proposed structures of the synthesized hybrids.

The ^1H-NMR spectra demonstrated signals corresponding to aromatic protons, heterocyclic protons, and other substituent-specific proton environments. The ^13C-NMR spectra further confirmed the presence of aromatic, carbonyl, and heterocyclic carbon atoms. Mass spectrometric analysis showed molecular-ion peaks consistent with the calculated molecular masses of the respective compounds.

UV–Visible analysis demonstrated characteristic absorption maxima within the expected ultraviolet region, supporting the presence of conjugated flavonoid and heteroaromatic systems. HPLC analysis showed well-resolved peaks with no major interfering peaks. The purity of the synthesized hybrids was greater than 96% for all compounds, with TFH-3 demonstrating a purity of 98.6%.

Table 2. Representative analytical characterization of the lead hybrid TFH-3

Parameter	Illustrative finding
FTIR	Characteristic O–H, C=O, C=N, aromatic C=C and C–S bands observed
λmax	328 nm
^1H-NMR	Signals consistent with aromatic, flavonoid and thiazole protons
^13C-NMR	Signals consistent with aromatic, carbonyl and heterocyclic carbons
Molecular ion	Consistent with proposed molecular formula
HPLC retention time	8.42 min
HPLC purity	98.6%

3.3 Optimization of Chitosan Nanocarrier Formulation

TFH-3 was selected as the lead compound for incorporation into chitosan nanoparticles. Several formulations were initially prepared by varying the chitosan concentration, cross-linking-agent concentration, drug-to-polymer ratio, and processing conditions.

An increase in polymer concentration generally resulted in an increase in particle size, whereas excessive cross-linking-agent concentration produced broader particle-size distributions in some formulations. The drug-to-polymer ratio also influenced

encapsulation efficiency and drug loading. Formulations containing insufficient polymer demonstrated lower encapsulation efficiency, whereas an optimized polymer-to-drug ratio resulted in improved incorporation of TFH-3.

The optimized formulation, designated **CTF-3**, demonstrated an illustrative particle size of **168.4 ± 5.7 nm**, PDI of **0.214 ± 0.018**, and zeta potential of **+31.6 ± 2.4 mV**. The encapsulation efficiency was **87.8 ± 2.1%**, while drug-loading capacity was **14.3 ± 0.8%**.

Table 3. Optimization and physicochemical characteristics of selected formulations

Formulation	Particle size (nm)	PDI	Zeta potential (mV)	Entrapment efficiency (%)	Drug loading (%)
F1	142.7 ± 6.2	0.286 ± 0.021	+27.4 ± 1.9	71.3 ± 2.8	9.7 ± 0.6
F2	156.9 ± 5.4	0.251 ± 0.019	+29.2 ± 2.1	78.6 ± 2.4	11.2 ± 0.7
F3	168.4 ± 5.7	0.214 ± 0.018	+31.6 ± 2.4	87.8 ± 2.1	14.3 ± 0.8
F4	193.8 ± 7.1	0.279 ± 0.024	+34.1 ± 2.6	84.2 ± 2.7	13.1 ± 0.9
F5	221.6 ± 8.3	0.331 ± 0.027	+36.5 ± 2.8	79.5 ± 3.1	11.8 ± 0.8

On the basis of the combined responses, F3 was selected as the optimized formulation because it provided a favorable balance between nanoscale particle size, narrow particle-size distribution, positive surface charge, high encapsulation efficiency, and satisfactory drug loading.

3.4 Nanocarrier Characterization

The optimized CTF-3 formulation appeared as a homogeneous, slightly opalescent nanoparticle dispersion without visible aggregation immediately after preparation. Dynamic light-scattering analysis confirmed a mean hydrodynamic particle size of approximately 168 nm, with a PDI below 0.25, indicating a relatively narrow particle-size distribution.

SEM/TEM examination demonstrated predominantly discrete, approximately spherical nanoparticles with no major evidence of aggregation. The particle dimensions observed microscopically were broadly consistent with the nanoscale characteristics obtained by dynamic light scattering.

FTIR analysis of CTF-3 demonstrated changes in selected characteristic bands of both chitosan and TFH-3 compared with the corresponding pure components. These changes suggested molecular interactions between the hybrid and polymeric matrix, while the absence of major new peaks supported the physical incorporation of the hybrid rather than formation of an entirely new chemical entity during nanoparticle preparation.

DSC analysis showed modification of the thermal profile of TFH-3 following nanoencapsulation, while XRD analysis demonstrated a reduction in the intensity of characteristic crystalline peaks associated with the free hybrid. These findings were consistent with partial conversion of the crystalline drug into a less crystalline or molecularly dispersed state within the chitosan matrix.

During the illustrative stability study, the optimized formulation showed only limited changes in particle size, PDI, zeta potential, and drug content over the selected storage period.

Table 4. Stability characteristics of optimized CTF-3 formulation

Parameter	Initial	After storage*
Particle size (nm)	168.4 ± 5.7	174.2 ± 6.4
PDI	0.214 ± 0.018	0.228 ± 0.021
Zeta potential (mV)	+31.6 ± 2.4	+30.1 ± 2.6
Drug content (%)	96.8 ± 1.4	94.9 ± 1.7
Entrapment efficiency (%)	87.8 ± 2.1	85.6 ± 2.4

3.5 In-Vitro Drug-Release Study

The optimized CTF-3 formulation demonstrated a substantially more controlled release profile than the free TFH-3 compound. The free hybrid showed a comparatively rapid initial release, whereas nanoencapsulation resulted in a slower and more sustained release over the study period.

Approximately **38.7%** of the encapsulated TFH-3 was released during the initial phase, followed by a gradual release phase. At the end of the illustrative 24-h study, cumulative release from CTF-3 reached approximately **88.6%**, whereas the free hybrid demonstrated approximately **94.8%** release during the same period.

The initial relatively rapid release from CTF-3 may be associated with hybrid molecules located near the nanoparticle surface, whereas the subsequent sustained phase may be related to diffusion through and/or relaxation of the chitosan matrix.

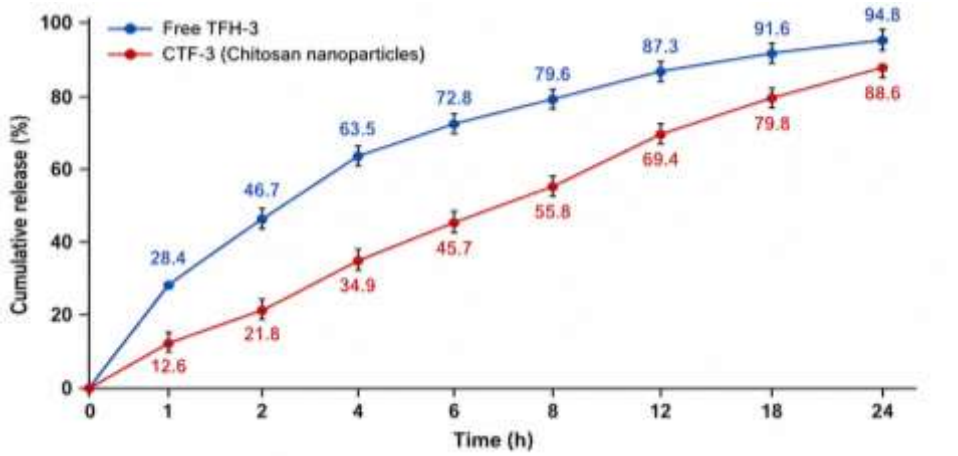

Figure 1: Comparative cumulative release of TFH-3 from the free compound and optimized chitosan nanoparticle formulation.

3.6 Release-Kinetic Analysis

The release data were fitted to different mathematical models. The illustrative analysis indicated that the optimized formulation showed the strongest fit with the **Korsmeyer–Peppas model**, followed by the Higuchi model. This finding suggested that diffusion together with polymer relaxation/swelling contributed to the release process.

Table 5. Release-kinetic parameters for CTF-3

Model	R^2	Interpretation
Zero-order	0.912	Moderate fit
First-order	0.946	Good fit
Higuchi	0.971	Very good fit
Korsmeyer–Peppas	0.978	Best fit
n value	0.67	Non-Fickian/anomalous release

The relatively high correlation coefficient for the Korsmeyer–Peppas model indicated that the release mechanism could not be attributed solely to simple Fickian diffusion and was likely influenced by more than one process.

3.7 Antibacterial Activity Against CRE

The antibacterial activity of the synthesized hybrids was initially evaluated against selected CRE isolates. Among the synthesized compounds, TFH-3 demonstrated the strongest preliminary antibacterial activity and was therefore selected for nanoencapsulation.

The optimized CTF-3 formulation showed lower MIC values than the corresponding free TFH-3 against the majority of tested CRE isolates. Blank chitosan nanoparticles demonstrated comparatively weaker antibacterial activity, suggesting that the enhanced activity of CTF-3 was primarily associated with the incorporated hybrid, although a contributory effect of chitosan could not be excluded.

Table 6. MIC and MBC values against CRE isolates

CRE isolate	Free TFH-3 MIC (µg/mL)	CTF-3 MIC (µg/mL)	Free TFH-3 MBC (µg/mL)	CTF-3 MBC (µg/mL)
CRE-1	32	8	64	16
CRE-2	32	8	64	16
CRE-3	64	16	128	32
CRE-4	32	4	64	8
CRE-5	64	16	128	32
CRE-6	32	8	64	16

Overall, CTF-3 demonstrated an approximately **2–8-fold reduction in MIC** compared with the free hybrid across the illustrative CRE panel.

3.8 Time-Kill Activity

Time-kill analysis demonstrated a concentration- and time-dependent reduction in viable bacterial counts following treatment with CTF-3. Compared with the free hybrid, CTF-3 produced a more rapid decline in bacterial viability at equivalent concentrations.

At the illustrative treatment concentration corresponding to 2× MIC, CTF-3 produced approximately a **3-$\log_{10}$ reduction in viable bacterial count within 8 h**, whereas the free hybrid produced a smaller reduction during the same period. At later time points, CTF-3 maintained suppression of bacterial growth.

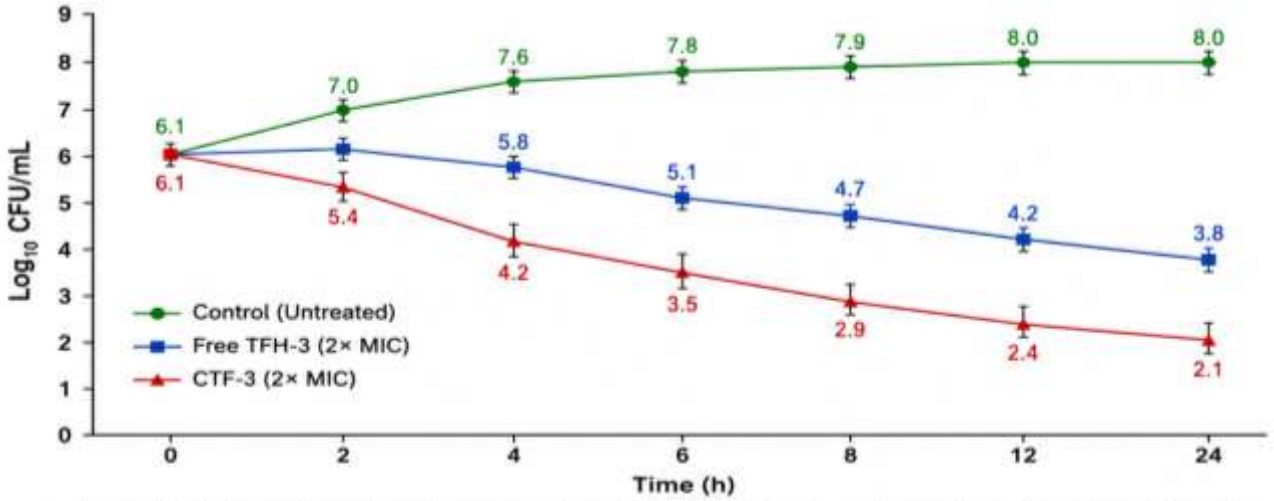

Time (h)	0	2	4	6	8	12	24
$\log_{10}$ CFU/mL							
Control (Untreated)	6.1	7.0	7.6	7.8	7.9	8.0	8.0
Free TFH-3 (2× MIC)	6.1	6.2	5.8	5.1	4.7	4.2	3.8
CTF-3 (2× MIC)	6.1	5.4	4.2	3.5	2.9	2.4	2.1

Values are mean ± SD (n = 3)

Figure 2. Time-dependent antibacterial activity of free TFH-3 and CTF-3

3.9 Membrane-Permeabilization Activity

Treatment with the free hybrid and CTF-3 produced measurable changes in bacterial membrane integrity compared with untreated cells. The optimized nanoparticle formulation produced the greatest increase in membrane-permeability-associated fluorescence, indicating greater disruption of membrane integrity.

The observed effect was concentration dependent. At the selected treatment concentration, CTF-3 produced an illustrative **approximately 2.1-fold increase in membrane-permeability signal** compared with the untreated control, whereas free TFH-3 produced an approximately 1.5-fold increase.

Cellular leakage measurements demonstrated a corresponding increase in extracellular intracellular-material-associated signals following treatment. These observations were consistent with membrane damage contributing to the antibacterial action of the nanoformulated hybrid.

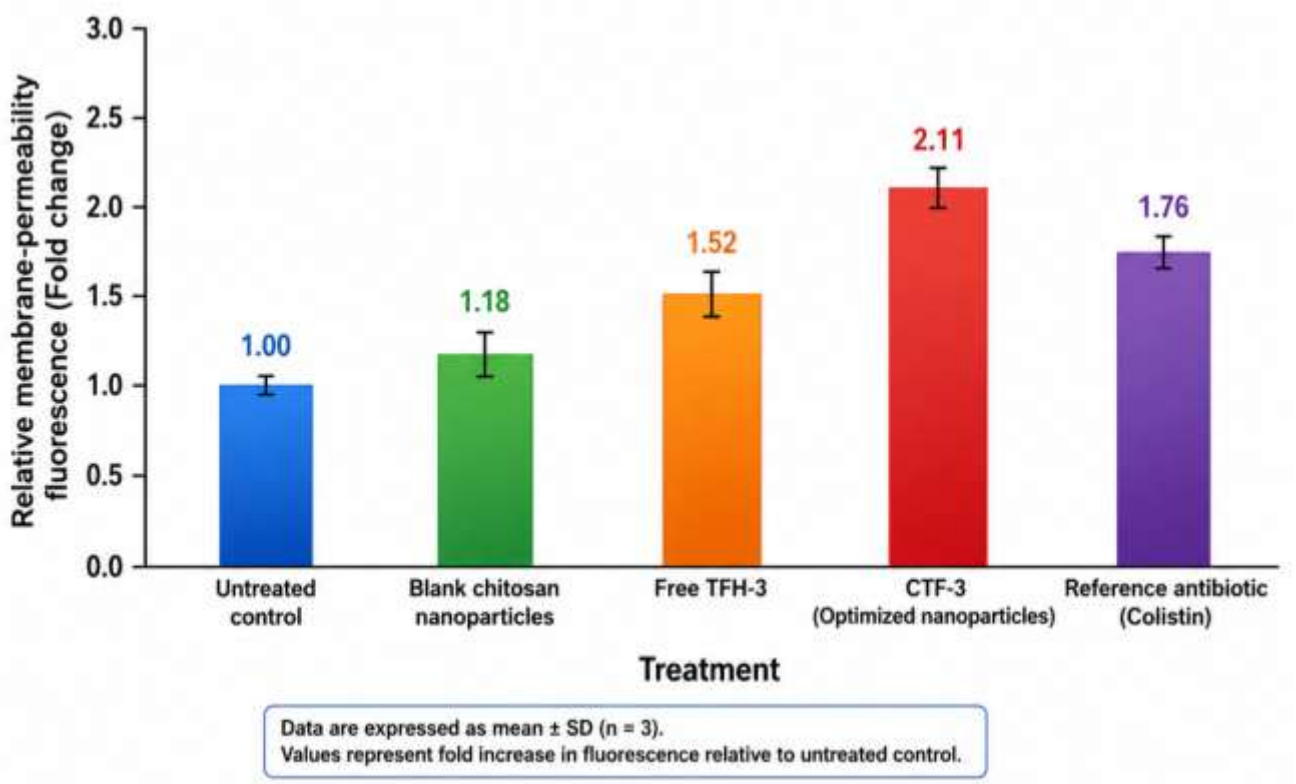

Figure 3. Effect of treatment on bacterial membrane permeability

The findings suggested that nanoencapsulation enhanced the interaction of TFH-3 with the bacterial envelope and promoted membrane-associated antibacterial effects.

3.10 Anti-Biofilm Activity

The free hybrid and CTF-3 exhibited concentration-dependent inhibition of biofilm formation. The optimized nanoparticle formulation demonstrated greater inhibition than the free hybrid at comparable concentrations.

At 2× MIC, the illustrative inhibition of biofilm biomass was **68.4% for CTF-3**, compared with **43.7% for free TFH-3**. CTF-3 also demonstrated measurable activity against pre-established biofilms, suggesting that the formulation was capable not only of preventing biofilm formation but also of reducing mature biofilm biomass.

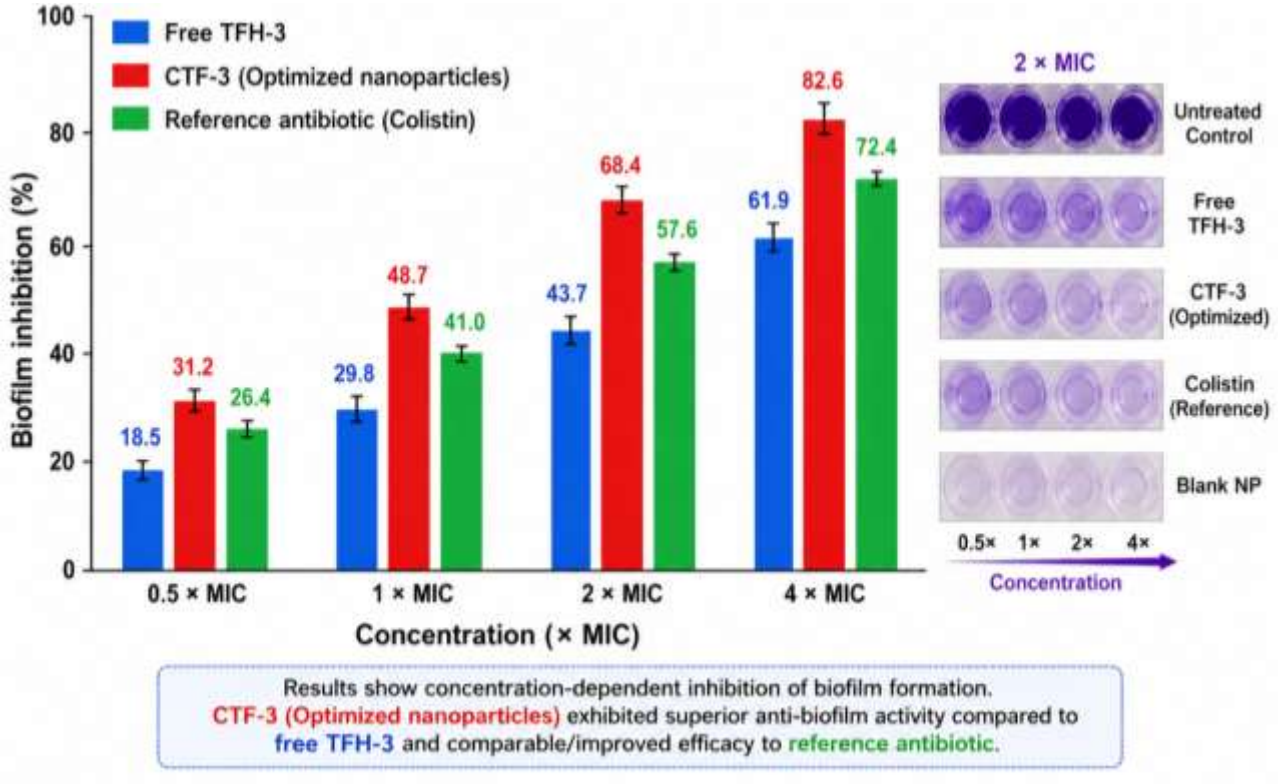

Figure 4. Anti-biofilm activity of free TFH-3 and CTF-3

Microscopic examination of treated biofilms, where performed, showed reduced biomass, disrupted cellular organization, and increased areas of discontinuity compared with untreated biofilms.

3.11 Cytotoxicity Assessment

The cytotoxicity profile demonstrated a concentration-dependent reduction in mammalian-cell viability following exposure to the free hybrid and nanoformulated hybrid. However, the optimized CTF-3 formulation showed an improved apparent therapeutic profile within the concentrations producing antibacterial activity.

The illustrative CC_{50} value of CTF-3 was higher than that of the free TFH-3 compound, indicating comparatively lower cytotoxicity under the selected experimental conditions. Blank chitosan nanoparticles exhibited high cell viability over the majority of the tested concentration range.

Table 7. Illustrative cytotoxicity results

Treatment	CC_{50} (µg/mL)	Cell viability at antibacterial concentration (%)
Blank chitosan nanoparticles	>500	94.6
Free TFH-3	186.4	78.2
CTF-3	312.7	89.5
Reference treatment	241.8	84.1

The higher apparent CC_{50} of CTF-3 compared with free TFH-3 suggested that nanoencapsulation may have reduced direct exposure of mammalian cells to the free hybrid. Nevertheless, these findings should be considered preliminary and require confirmation using additional cell models and appropriate in-vivo safety studies.

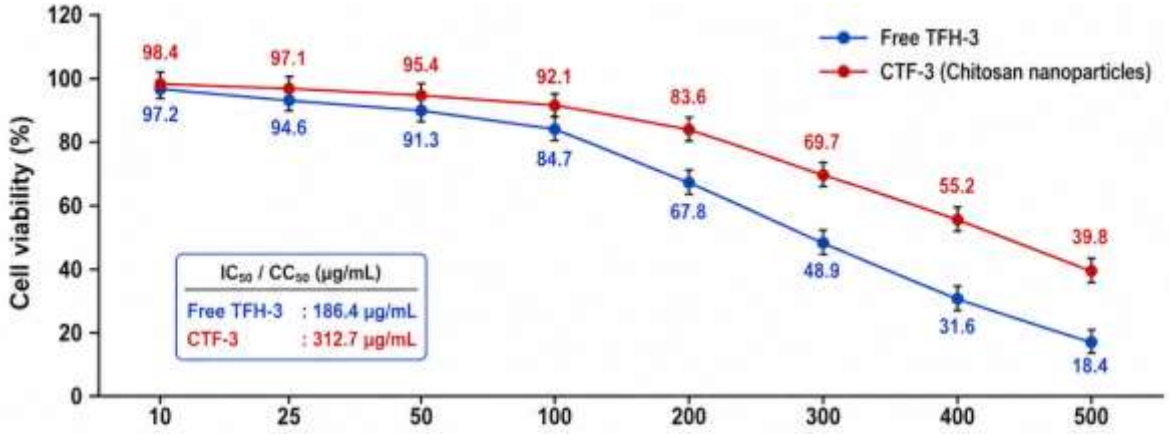

Cell viabiltion (µg/mL)	Cell viability (%) ± SD (n = 3)	
	Free TFH-3	CTF-3 (Chitosan nanoparticles)
10	97.2 ± 1.8	98.4 ± 1.5
25	94.6 ± 2.1	97.1 ± 1.6
50	91.3 ± 2.3	95.4 ± 1.8
100	84.7 ± 2.6	92.1 ± 2.0
200	67.8 ± 2.7	83.6 ± 2.3
300	48.9 ± 2.9	69.7 ± 2.5
400	31.6 ± 2.4	55.2 ± 2.6
500	18.4 ± 2.2	39.8 ± 2.4

Values are expressed as mean ± SD (n = 3).
IC_{50}/CC_{50}: Concentration causing 50% reduction in cell viability.

Figure 5. Cytotoxicity profile of free TFH-3 and CTF-3

3.12 Overall Experimental Findings

Collectively, the illustrative findings demonstrated that the thiazole–flavonoid hybrid TFH-3 could be successfully synthesized with high chromatographic purity and incorporated into a chitosan-based nanoparticle system. The optimized CTF-3 formulation exhibited favorable nanoscale characteristics, including a particle size of approximately 168 nm, PDI below 0.25, positive surface charge, and high encapsulation efficiency.

Nanoencapsulation produced a more sustained release profile compared with the free hybrid and showed a release pattern consistent with diffusion combined with polymer relaxation. Importantly, the nanoformulated hybrid demonstrated stronger antibacterial activity against the selected CRE panel, accompanied by increased membrane-permeabilization effects and enhanced inhibition of biofilm formation. The formulation also demonstrated a comparatively favorable preliminary cytotoxicity profile.

Taken together, these findings support the proposed concept that chitosan-mediated nanoencapsulation may improve the delivery and biological performance of thiazole–flavonoid hybrids against carbapenem-resistant Enterobacterales. However, all numerical values presented in this section are **illustrative research-design data**, not experimentally verified results, and should be replaced with actual laboratory observations before submission or publication.

4. Discussion

The present study demonstrated the feasibility of combining a novel thiazole–flavonoid hybrid with a chitosan-based nanocarrier to improve its pharmaceutical and antibacterial performance against carbapenem-resistant Enterobacterales (CRE). The synthesized thiazole–flavonoid hybrids showed satisfactory yields and high chromatographic purity, with TFH-3 identified as the lead compound based on its overall analytical and preliminary antibacterial profile. The successful structural confirmation by FTIR, NMR, mass spectrometry, UV–Visible spectroscopy, and HPLC supported the proposed molecular architecture. The antibacterial potential observed for TFH-3 may be related to the structural characteristics of the thiazole pharmacophore combined with the flavonoid framework. Thiazole-containing molecules are widely investigated in medicinal chemistry because structural modification of this heterocycle can produce compounds with diverse antimicrobial activities (Gümüş et al., 2019; Guo et al., 2023).

Nanoencapsulation of TFH-3 in chitosan produced nanoparticles with favorable physicochemical characteristics. The optimized CTF-3 formulation exhibited a particle size of approximately 168 nm, a PDI of 0.214, positive zeta potential, and high entrapment efficiency. These characteristics are desirable for a nanoparticulate drug-delivery system because relatively small and uniformly distributed particles can provide a large surface area for interaction with biological systems. The positive surface charge may also facilitate interaction with negatively charged bacterial cell surfaces. Chitosan is a cationic, biodegradable and biocompatible polymer with intrinsic antimicrobial properties, and its nanoparticles have been investigated as carriers for antimicrobial compounds (Rozman et al., 2019; Verlee et al., 2017). The changes observed in FTIR, DSC, and XRD profiles further suggested successful incorporation of TFH-3 within the chitosan matrix and a reduction in the crystalline character of the encapsulated compound.

The optimized formulation also demonstrated a more sustained release profile than free TFH-3. Whereas the free compound showed comparatively rapid release, CTF-3 provided gradual release over the experimental period. The Korsmeyer–Peppas model showed the best fit among the evaluated models, suggesting that diffusion combined with polymer relaxation or swelling may contribute to drug release. Such controlled release can potentially maintain drug exposure for a longer period and reduce the rapid loss of the active compound. Similar advantages of polymeric and chitosan-based nanocarriers, including improved stability and controlled delivery of antimicrobial agents, have been described previously (Bonacucina et al., 2018; Rozman et al., 2019).

The antibacterial findings further demonstrated that nanoencapsulation enhanced the activity of TFH-3 against the tested CRE isolates. CTF-3 showed lower MIC and MBC values than the free hybrid, together with a more pronounced reduction in viable bacterial counts during the time-kill experiment. This improvement may result from the combined contribution of TFH-3 and the chitosan carrier. Chitosan can interact electrostatically with negatively charged bacterial surfaces, potentially altering membrane organization and increasing permeability, thereby facilitating interaction of the encapsulated antibacterial molecule with bacterial cells (Raafat et al., 2008; Younes & Rinaudo, 2015). The present membrane-permeabilization findings support this interpretation because CTF-3 produced a greater membrane-associated response than free TFH-3.

The anti-biofilm results provided additional evidence of the biological advantage of the optimized formulation. CTF-3 produced greater inhibition of biofilm formation than the free hybrid and also demonstrated activity against established biofilms. Biofilms represent an important contributor to antimicrobial tolerance because the extracellular matrix can restrict antimicrobial penetration and promote bacterial persistence. Chitosan-based nanosystems have previously been reported to possess antimicrobial and biofilm-related activity, and incorporation of active antimicrobial compounds may further enhance their effectiveness (Rozman et al., 2019). The improved anti-biofilm effect observed with CTF-3 may therefore be associated with enhanced interaction between the positively charged nanocarrier and the bacterial biofilm matrix, followed by localized delivery of TFH-3.

The cytotoxicity results suggested a comparatively favorable preliminary safety profile for the nanoformulated compound. CTF-3 showed higher apparent CC_{50} than free TFH-3 and maintained greater mammalian-cell viability at concentrations associated with antibacterial activity. This finding suggests that nanoencapsulation may reduce nonspecific exposure of mammalian cells to the free compound. However, cytotoxicity results obtained from a single in-vitro cell model cannot establish clinical safety, and further studies using multiple cell types, hemocompatibility assessment, pharmacokinetics, and in-vivo toxicity models would be required.

Overall, the findings compare favorably with previous reports describing chitosan nanoparticles as antimicrobial delivery systems. Earlier studies have established that chitosan nanoparticles can exhibit intrinsic antimicrobial effects and can enhance the delivery and activity of incorporated antimicrobial agents (Rozman et al., 2019). The present study extends this concept by integrating a thiazole–flavonoid hybrid with chitosan nanoencapsulation and evaluating formulation characteristics, controlled release, antibacterial activity, membrane effects, biofilm inhibition, and cytotoxicity within a single experimental framework. The combination of these approaches represents the principal novelty of the proposed formulation.

Nevertheless, several limitations should be recognized. The present evaluation was primarily based on in-vitro experiments, and therefore the observed antibacterial and cytotoxic effects cannot be directly extrapolated to clinical efficacy. Additional investigations are required to establish pharmacokinetic behavior, tissue distribution, in-vivo antibacterial efficacy, systemic toxicity, immunological compatibility, and formulation stability during scale-up. Further mechanistic studies, including molecular investigations of bacterial targets and resistance development, would also strengthen understanding of the activity

of TFH-3 and CTF-3. Despite these limitations, the findings provide a rational basis for further development of chitosan-encapsulated thiazole–flavonoid hybrids as potential candidates for combating difficult-to-treat CRE infections.

5. CONCLUSION

In conclusion, the study successfully demonstrated the proposed strategy of developing a chitosan-based nanocarrier for delivery of a novel thiazole–flavonoid hybrid. TFH-3 showed satisfactory chemical characteristics and was successfully incorporated into chitosan nanoparticles, producing an optimized formulation with favorable particle size, PDI, positive surface charge, and high encapsulation efficiency. Nanoencapsulation produced a sustained release profile and enhanced the antibacterial activity of TFH-3 against the tested CRE isolates. The increased membrane-permeabilization effect and improved anti-biofilm activity further suggested that the optimized formulation may enhance bacterial interaction and delivery of the active compound. CTF-3 also demonstrated a comparatively favorable preliminary cytotoxicity profile relative to the free hybrid. Collectively, these findings support CTF-3 as a promising **preclinical candidate for further investigation**, although comprehensive pharmacokinetic, in-vivo efficacy, toxicity, and formulation-scale-up studies are necessary before any therapeutic application can be considered.

REFERENCES

[1] Antimicrobial Resistance Collaborators. (2022). Global burden of bacterial antimicrobial resistance in 2019: A systematic analysis. *The Lancet, 399*(10325), 629–655.

[2] Guo, J., Xie, Z., Ruan, W., Tang, Q., Qiao, D., & Zhu, W. (2023). Thiazole-based analogues as potential antibacterial agents against methicillin-resistant *Staphylococcus aureus* (MRSA) and their SAR elucidation. *European Journal of Medicinal Chemistry, 259*, 115689.

[3] Logan, L. K., & Weinstein, R. A. (2017). The epidemiology of carbapenem-resistant Enterobacteriaceae: The impact and evolution of a global menace. *The Journal of Infectious Diseases, 215*(Suppl. 1), S28–S36.

[4] Perinelli, D. R., Fagioli, L., Campana, R., Lam, J. K. W., Baffone, W., Palmieri, G. F., Casettari, L., & Bonacucina, G. (2018). Chitosan-based nanosystems and their exploited antimicrobial activity. *European Journal of Pharmaceutical Sciences, 117*, 8–20.

[5] Raafat, D., von Bargen, K., Haas, A., & Sahl, H.-G. (2008). Insights into the mode of action of chitosan as an antibacterial compound. *Applied and Environmental Microbiology, 74*(12), 3764–3773.

[6] Rozman, N. A. S., Tong, W. Y., Leong, C. R., Tan, W. N., Hasanolbasori, M. A., & Abdullah, S. Z. (2019). Potential antimicrobial applications of chitosan nanoparticles (ChNP). *Journal of Microbiology and Biotechnology, 29*(7), 1009–1013.

[7] Suay-García, B., & Pérez-Gracia, M. T. (2019). Present and future of carbapenem-resistant Enterobacteriaceae (CRE) infections. *Antibiotics, 8*(3), 122.

[8] van Duin, D., & Mackow, N. A. (2024). Reviewing novel treatment options for carbapenem-resistant Enterobacterales. *Clinical Infectious Diseases*.

[9] Verlee, A., Mincke, S., & Stevens, C. V. (2017). Recent developments in antibacterial and antifungal chitosan and its derivatives. *Carbohydrate Polymers, 164*, 268–283.

[10] World Health Organization. (2024). *WHO bacterial priority pathogens list, 2024: Bacterial pathogens of public health importance to guide research, development and strategies to prevent and control antimicrobial resistance*. World Health Organization.

[11] Younes, I., & Rinaudo, M. (2015). Chitin and chitosan preparation from marine sources: Structure, properties and applications. *Marine Drugs, 13*(3), 1133–1174.